http://bilimseldergiler.atauni.edu.tr/system/index.php/physics-astronomy/index
ISSN:
Atatürk Üniversitesi
Anadolu Fizik ve Astronomi Dergisi (ISSN: 2791-8718)
Cilt 1, Sayı 2, 46-64, 2021

Atatürk University
Journal of Anatolian Physics and Astronomy (ISSN: 2791-8718)
Volume 1, Issue 2, 46-64, 2021

JAPA

INVESTIGATION OF SOME PROPERTIES OF 4-AMINO-2-METHYL-7 (TRIFLUOROMETHYL) QUINOLINE MOLECULE BY EXPERIMENTAL AND THEORETICAL SPECTROSCOPIC METHODS

Tevfik Raci Sertbakan[*1]

[1]University of Kırşehir Ahi Evran, Faculty of Art and Science, Physics Department, Kırşehir, Turkey

(Alınış / Received: 05.05.2021, Kabul / Accepted: 27.05.2021, Online Yayınlanma / Published Online: 31.12.2021)

*Corresponding Author: trsertbakan@ahievran.edu.tr (T.R. Sertbakan)
(ORCID: https://orcid.org/0000-0001-7264-4399)

Keywords
4-amino-2-methyl-7(trifluoromethyl)quinolone,
FT-IR Spectra,
Raman Spectra ,
NMR Spectra,
Density Functional Theory (DFT).

Abstract: In this study, the theoretical calculations of the 4-amino-2-methyl-7(trifluoromethyl)quinoline molecule (Abbr. AM7TFMQ) were made using the B3LYP method and the basis sets cc-pVDZ and 6-311G(d,p) in Gaussian09 program, which is a Density Function Theory (DFT) software. These calculations were made in the gas phase of the molecule. To find the most stable conformation of the AM7TFMQ molecule, the theoretical methods included in the Gaussian09 package program were used. Harmonic vibration frequencies of the molecule were calculated using similar methods and basis sets in the same program. These calculated frequencies were scaled. Then, Infrared and Raman spectroscopy techniques were used for experimental comparison. These vibrational modes were plotted on the 6-311G(d,p) basis set using the SQM program based on TED analysis. It has been observed that these calculated frequencies are quite compatible with the observed values. The highest energy occupied molecular orbital (HOMO) and the lowest energy unoccupied molecular orbital (LUMO) energies of the AM7TFMQ molecule were detected. It can be said that the transitions in these molecular orbitals occur due to the charge transfers in the molecule. Additionally, the molecular electrostatic potential (MEP) maps of the AM7TFMQ molecule were draw by the DFT method. The experimental ^{1}H and ^{13}C chemical shifts were observed by taking NMR spectrum in dimethyl sulfoxide solution. These shifts were theoretically calculated using gauge including atomic orbital (GIAO–The Gauge Invariant Atomic Orbitals) shielding tensors. Our experimental and theoretical NMR results are highly compatible.

4-AMİNO-2-METİL-7(TRİFLOROMETİL)KİNOLİN MOLEKÜLÜNÜN BAZI ÖZELLİKLERİNİN DENEYSEL VE TEORİK SPEKTROSKOPİK YÖNTEMLERLE İNCELENMESİ

Anahtar Kelimeler
4-amino-2-metil-7(triflorometil)kinolin,
FT-IR Spektrum,
Raman Spektrum,
NMR Spektrum,
Density Functional Theory (DFT)

Özet: Bu çalışmada, 4-amino-2-metil-7(triflorometil)kinolin molekülünün (Kısaltma. AM7TFMQ) teorik hesaplamaları B3LYP yöntemi ve cc-pVDZ ve 6-311G(d,p) temel setleri kullanılarak Yoğunluk Fonksiyonu Teorisi (DFT) yazılımı olan Gaussian09 programında yapılmıştır. Bu hesaplamalar molekülün gaz fazında yapıldı. AM7TFMQ molekülünün en kararlı yapısını bulmak için Gaussian09 paket programında yer alan teorik yöntemler kullanıldı. Molekülün harmonik titreşim frekansları, aynı programda benzer yöntemler ve temel setler kullanılarak hesaplanmıştır. Hesaplanan bu frekanslar ölçeklendi. Daha sonra deneysel karşılaştırma için Kızılötesi ve Raman spektroskopi teknikleri kullanılmıştır. Bu titreşim modları, TED analizine dayalı SQM programı kullanılarak 6-311G(d,p) temel setine göre çizilmiştir. Hesaplanan bu frekansların gözlenen değerlerle oldukça uyumlu olduğu görülmüştür. AM7TFMQ molekülünün en yüksek enerjili moleküler orbital (HOMO) ve en düşük enerjili boş moleküler orbital (LUMO)

enerjileri tespit edildi. Moleküler orbitallerdeki geçişlerin molekül içindeki yük transferlerinden dolayı meydana geldiği söylenebilir. Ek olarak, AM7TFMQ molekülünün moleküler elektrostatik potansiyel (MEP) haritaları DFT yöntemi ile çizildi. Dimetil sülfoksit çözeltisi içinde NMR spektrumu alınarak deneysel 1H ve 13C kimyasal kaymaları gözlemlendi. Bu kaymalar teorik olarak, atomik orbital (GIAO – The Gauge Invariant Atomic Orbitaller) koruyucu tensörleri içeren gösterge kullanılarak hesaplandı. Deneysel ve teorik NMR sonuçlarımız oldukça uyumludur.

1. Introduction

The quinoline ring is a ring that attracts the attention of scientists because it is involved in the construction of some natural products and some compounds showing various biological activities [1,2]. This molecule contains pyridine and benzene molecules coupled from two carbon atoms. It is therefore a compound of aromatic nitrogen [3]. Having many pharmaceutical and biological applications, quinoline molecule is found in bone mineral and coal tar [4]. It use as a metal extraction material [5]. Other properties of quinoline derivatives investigated in the literature are their antineoplastic and cardiovascular activities [6,7]. Quinoline derivatives have several vital roles in various functions [8,9]. This vital role can be listed as antifilarial [10] antibacterial [11,12] and antimalarial activities [13-15]. For this reason, the spectroscopic characterization of these structures is very important. Therefore, experimental and theoretical IR and Raman spectroscopy studies of quinoline derivatives have been carried out. In addition, many studies have investigated the spectral and structural properties of these molecules [16-18]. The studied molecule 4-amino-2-methyl-7(trifluoromethyl)quinolone (AM7TFMQ) is a quinoline derivative containing three fluorine atoms together with amino and methyl groups. In the literature, the X-ray data study that gives the geometric parameters of this molecule has not been found. I did the spectroscopic studies of the AM7TFMQ molecule for the first time. I also compared our title molecule with the 4-amino-2-methyl-8(trifluoromethyl)quinoline (AM8TFMQ) molecule, which had previously entered the literature and was very similar to the title molecule. [19]. In this article, the theoretical and experimental studies on Infrared, Raman and NMR spectra were carried out and compared with the results reported in Ref. [19] and [30]. In addition, the theoretical HOMO-LUMO calculations have been made and the MEPs maps are drawn for our molecules.

2. Experimental Details

The AM7TFMQ compound ($C_{11}H_9F_3N_2$, 226.2 g/mol, dirty white color powder) was purchased from Sigma-Aldrich chemical company in 1 g package. The FT-IR spectrum of the AM7TFMQ molecule was taken by pellet method in the KBr window at 4000-500 cm^{-1} region at room temperature using Perkin-Elmer Spectrum One FT-IR spectrometer. The Raman spectrum of our molecule was taken using a Thermo Scientific DXR Raman Microscope with Nd: YVO4 DPSS Raman Spectrophotometer, which was stimulated with 532 nm laser at 4000-50 cm^{-1} region. ^{1}H and ^{13}C NMR spectra of this molecule were taken in dimethylsulfoxide (DMSO) solution in a tetramethylsilane (TMS) calorimeter at 25 ° C using a Bruker DPX 400 MHz NMR spectrometer.

3. Computational Details

I first carried out the optimization process of the AM7TFMQ molecule using B3LYP functional and cc-pVDZ and 6-311G(d,p) basis sets in this work. The geometry of the optimized AM7TFMQ molecule is given in **Figure 1.** Using Density Functional Theory (DFT), geometric parameters of the molecule such as bond distance, bond angles, dihedral angles and vibrational frequencies were calculated. This frequencies of the molecule were fitted to the experimental observations by multiplying the scale factors of the basis sets by 0.970 for cc-pVDZ and 0.966 for 6-311G(d,p). Moreover, the obtained vibrational modes were assignment by TED analysis in the frame of SQM program [20]. Then all geometric parameters calculated were compared with the experimental values obtained. On the other hand, the ^{1}H and ^{13}C NMR isotropic shielding tensors of AM7TFMQ molecule were calculated by the GIAO method, which is one of the most common approaches in this matter [21,22]. Moreover, the HOMO-LUMO energies of the molecule were calculated by the B3LYP method of time independent density function theory (TD-DFT) [23-26] using the optimized structure. Because this DFT method can calculate the ground state energies of materials well [27,28].

Finally, the Molecular Electrostatic Potential (MEP) Surfaces of the title molecule were calculated. Thus, the reactive regions of this molecule were also investigated. All calculations were performed by Gaussian09 packet program [29].

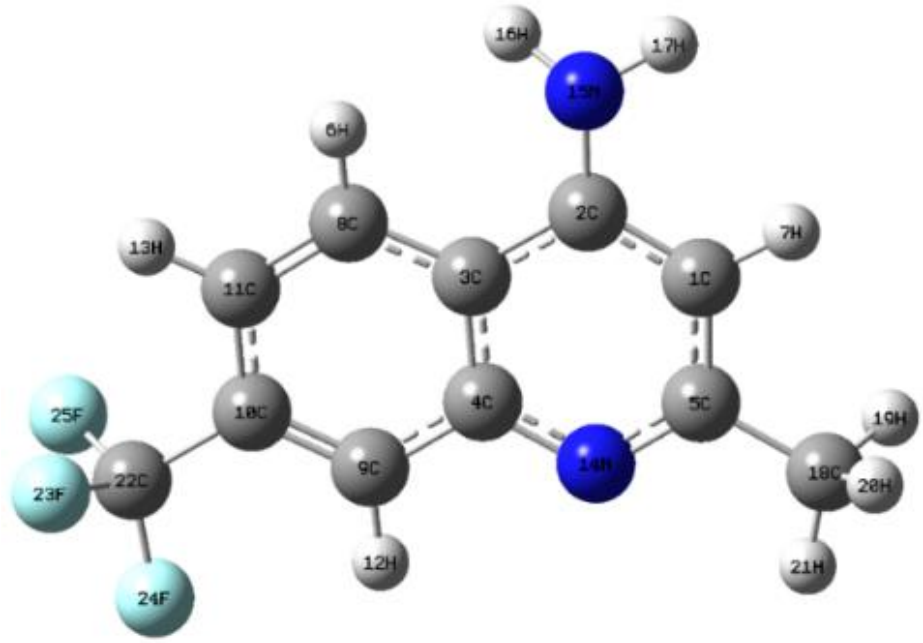

Figure 1. The most stable geometry of the 4-amino-2-methyl-7(trifluoromethyl)quinoline molecule

4. Results and Discussion

4.1. Geometric Parameters

The geometric parameters of the AM7TFMQ molecule, such as the distance between its atoms, bond angles and dihedral angles were calculated using the basic sets of cc-pVDZ and 6-311G(d,p). The results are given in **Table 1**. I had previously worked with the AM8TFMQ molecule, which is very similar to the molecule in this study [19]. Also, a molecular spectroscopic study of the 4-amino-2-methylquinoline (AMQ) molecule similar to our molecule is available in the literature [30]. I compared the geometric parameters I calculated with the geometric parameters of the molecules in these two studies in **Table 1.** As a result of these comparisons, I observed a very good fit.

C–C bond lengths in the benzene ring were found to be in the range of 1.373–1.432 Å. The lowest value of these lengths is 1.373 Å between C_8–C_{11} atoms, and the largest value is 1.432 Å between C_3–C_4 atoms. Looking at the C– H bond lengths in the same ring, it is seen that there are values between 1.082–1.092 Å. C–C bond lengths in the pyridine ring were calculated between 1.383–1.440 Å values.

The only C–H bond in this ring is the C_1–H_7 bond. The length of this bond was calculated as 1.085 Å and 1.093 Å for two different basic sets. In my calculations, it has been observed that the bond lengths of N_{15}–H_{16} and N_{15}–H_{17} in the aniline group are in the range 1.007–1.015 Å. In addition, C–H bond lengths in the methyl group were calculated in the range of 1.089–1,103 Å. Finally, it was found as a result of the calculations that the lengths of three C–F bonds were between 1.347–1.358 Å.

All these calculations related to bond lengths are shown in Table S1. The calculated bond length values are quite compatible with the bond length values for the molecules in the reference studies. It can be thought that the very small differences that appear are the CF_3 group and the binding sites that bind to the molecules. In other words, due to this difference in the attachment point of the CF_3 group, the mass center of our molecule has changed and these small differences have resulted; can be interpreted as.

The angles between the C–C–C bonds in the benzene ring are in the order of 120^0 degrees. C–C–C and C–C–N angles not adjacent to benzene in the pyridine ring were calculated greater than 120^0 degrees. The C–C–C angles of the pyridine ring adjacent to the benzene were calculated as 117^0 degrees while the C–C–N angles were calculated as large as 120^0 degrees. It is also seen from the table that there is 117^0 degrees in the C_4–N_{14}–C_5 angle in the pyridine ring.

Table 1. Optimized geometric parameters of 4-amino-2-methyl-7(trifluoromethyl)quinoline (B3LYP)

Bond Lengths (Å)	**cc-pVDZ**	**6-311G(d,p)**	**cc-pVDZ[19]**	**6-311G++(d,p)[30]**
C_1-C_2	1.387	1.383	1.387	1.38
C_1-C_5	1.419	1.414	1.417	1.42
C_1-H_7	1.093	1.085	1.093	1.08
C_2-C_3	1.439	1.435	1.440	1.43
C_2-N_{15}	1.384	1.380	1.384	1.38
C_3-C_4	1.429	1.426	1.432	1.43
C_3-C_8	1.421	1.417	1.418	1.42
C_4-C_9	1.422	1.419	1.432	1.42
C_4-N_{14}	1.366	1.362	1.362	1.36
C_5-N_{14}	1.324	1.320	1.364	1.32
C_5-C_{18}	1.508	1.507	1.508	1.51
H_6-C_8	1.092	1.084	1.092	1.08
C_8-C_{11}	1.378	1.373	1.380	1.38
C_9-C_{10}	1.379	1.374	1.382	1.38
C_9-H_{12}	1.089	1.082	1.089	1.08
C_{10}-C_{11}	1.419	1.415	1.412	1.41
C_{10}-C_{22}	1.505	1.504	1.512	-
C_{11}-H_{13}	1.091	1.083	1.091	1.08
N_{15}-H_{16}	1.014	1.007	1.014	1.01
N_{15}-H_{17}	1.015	1.008	1.015	1.01
C_{18}-H_{19}	1.103	1.095	1.103	1.09
C_{18}-H_{20}	1.103	1.095	1.103	1.09
C_{18}-H_{21}	1.097	1.089	1.097	1.09
C_{22}-F_{23}	1.356	1.356	1.348	-
C_{22}-F_{24}	1.349	1.347	1.349	-
C_{22}-F_{25}	1.356	1.358	1.361	-
Bond Angels(º)	**cc-pVDZ**	**6-311G(d,p)**	**cc-pVDZ[19]**	**6-311G++(d,p)[30]**
C_2-C_1-C_5	120.626	120.692	120.3	120.54
C_2-C_1-H_7	119.894	119.960	119.9	120.02
C_5-C_1-H_7	119.476	119.347	119.6	119.44
C_1-C_2-C_3	117.469	117.624	117.7	117.82
C_1-C_2-N_{15}	121.960	121.497	121.7	121.40
C_3-C_2-N_{15}	120.515	120.833	120.4	120.74
C_2-C_3-C_4	117.192	117.073	117.1	117.08
C_2-C_3-C_8	123.634	123.840	123.1	123.80
C_4-C_3-C_8	119.171	119.087	119.6	119.12
C_3-C_4-C_9	118.628	118.726	118.0	118.58
C_3-C_4-N_{14}	123.961	123.823	123.5	123.57
C_9-C_4-N_{14}	117.410	117.450	118.3	117.85
C_1-C_5-N_{14}	123.296	123.031	123.2	123.11
N_{14}-C_5-C_{18}	117.162	117.458	117.0	117.44
C_3-C_8-H_6	120.105	120.404	119.9	120.28
C_3-C_8-C_{11}	121.038	121.106	121.7	120.88
H_6-C_8-C_{11}	118.840	118.479	119.1	118.83
C_4-C_9-C_{10}	120.827	120.679	120.0	121.03
C_4-C_9-H_{12}	117.468	117.644	119.3	117.30
C_{10}-C_9-H_{12}	121.704	121.677	119.8	121.67
C_9-C_{10}-C_{11}	120.567	120.722	120.7	120.31
C_9-C_{10}-C_{22}	121.104	121.002	119.7	120.03
C_{11}-C_{10}-C_{22}	118.329	118.276	119.5	119.65
C_8-C_{11}-C_{10}	119.743	119.668	120.0	120.07
C_8-C_{11}-H_{13}	120.480	120.392	120.3	120.02
C_{10}-C_{11}-H_{13}	119.775	119.938	119.6	119.91
C_4-N_{14}-C_5	117.425	117.739	117.8	117.87
C_2-N_{15}-H_{16}	116.276	118.182	116.2	116.89
C_2-N_{15}-H_{17}	115.225	116.642	115.0	116.89

Table 1. (Continue)

H_{16}-N_{15}-H_{17}	111.965	113.615	111.8	113.27
C_5-C_{18}-H_{19}	111.111	111.031	110.8	110.56
C_5-C_{18}-H_{20}	110.946	110.860	111.0	110.56
C_5-C_{18}-H_{21}	109.670	109.732	109.6	110.56
H_{19}-C_{18}-H_{20}	107.059	107.310	107.0	108.36
H_{19}-C_{18}-H_{21}	109.024	108.966	108.9	108.36
H_{20}-C_{18}-H_{21}	108.961	108.875	109.1	108.36
C_{10}-C_{22}-F_{23}	111.536	111.686	112.5	-
C_{10}-C_{22}-F_{24}	112.851	113.052	112.5	-
C_{10}-C_{22}-F_{25}	111.433	111.594	111.0	-
F_{23}-C_{22}-F_{24}	107.261	107.040	107.5	-
F_{23}-C_{22}-F_{25}	106.198	106.081	106.3	-
F_{24}-C_{22}-F_{25}	107.202	106.982	106.3	-
DihedralAngels(º)	**cc-pVDZ**	**6-311G(d,p)**	**cc-pVDZ[19]**	**6-311G++(d,p)[30]**
C_5-C_1-C_2-C_3	0.880	0.647	-0.999	-
C_5-C_1-C_2-N_{15}	178.182	178.203	-178.2	-
H_7-C_1-C_2-C_3	-179.863	-179.725	179.8	-
H_7-C_1-C_2-N_{15}	-2.561	-2.170	2.531	-
C_2-C_1-C_5-N_{14}	0.703	0.524	-0.727	-
C_2-C_1-C_5-C_{18}	-179.970	-179.859	179.9	-
H_7-C_1-C_5-N_{14}	-178.557	-179.106	178.4	-
H_7-C_1-C_5-C_{18}	0.770	0.511	-0.887	-
C_1-C_2-C_3-C_4	-1.864	-1.426	2.055	-
C_1-C_2-C_3-C_8	177.494	178.341	-177.2	-
N_{15}-C_2-C_3-C_4	-179.206	-178.999	179.3	-
N_{15}-C_2-C_3-C_8	0.152	0.768	0.093	-
C_1-C_2-N_{15}-H_{16}	150.101	156.083	-149.4	-
C_1-C_2-N_{15}-H_{17}	16.178	15.075	-15.91	-
C_3-C_2-N_{15}-H_{16}	-32.678	-26.439	33.31	-
C_3-C_2-N_{15}-H_{17}	-166.601	-167.447	166.88	-
C_2-C_3-C_4-C_9	-178.783	-179.024	178.7	-
C_2-C_3-C_4-N_{14}	1.501	1.214	-1.629	-
C_8-C_3-C_4-C_9	1.829	1.198	-1.982	-
C_8-C_3-C_4-N_{14}	-177.888	-178.565	177.6	-
C_2-C_3-C_8-H_6	-2.430	-2.024	2.444	-
C_2-C_3-C_8-C_{11}	179.085	179.206	-179.0	-
C_4-C_3-C_8-H_6	176.916	177.739	-176.8	-
C_4-C_3-C_8-C_{11}	-1.569	-1.031	1.647	-
C_3-C_4-C_9-C_{10}	-0.827	-0.538	0.987	-
C_3-C_4-C_9-H_{12}	179.467	179.645	-179.2	-
N_{14}-C_4-C_9-C_{10}	178.908	179.239	-178.6	-
N_{14}-C_4-C_9-H_{12}	-0.798	-0.574	1.015	-
C_3-C_4-N_{14}-C_5	0.017	-0.092	-0.026	-
C_9-C_4-N_{14}-C_5	-179.703	-179.857	179.6	-
C_1-C_5-N_{14}-C_4	-1.152	-0.804	1.244	-
C_{18}-C_5-N_{14}-C_4	179.506	179.572	-179.3	-
C_1-C_5-C_{18}-H_{19}	-57.852	-57.756	-61.64	-
C_1-C_5-C_{18}-H_{20}	61.128	61.430	57.27	-
C_1-C_5-C_{18}-H_{21}	-178.454	-178.274	177.9	-
N_{14}-C_5-C_{18}-H_{19}	121.516	121.882	118.9	-
N_{14}-C_5-C_{18}-H_{20}	-119.504	-118.932	-122.1	-
N_{14}-C_5-C_{18}-H_{21}	0.914	1.364	-1.427	-
C_3-C_8-C_{11}-C_{10}	0.259	0.175	-0.255	-
C_3-C_8-C_{11}-H_{13}	179.666	179.699	-179.7	-
H_6-C_8-C_{11}-C_{10}	-178.244	-178.618	178.2	-
H_6-C_8-C_{11}-H_{13}	1.162	0.907	-1.267	-
C_4-C_9-C_{10}-C_{11}	-0.487	-0.323	0.388	-
C_4-C_9-C_{10}-C_{22}	179.709	179.692	179.8	-
H_{12}-C_9-C_{10}-C_{11}	179.206	179.482	-179.3	-

Table 1. (Continue)

H_{12}-C_9-C_{10}-C_{22}	-0.597	-0.503	0.125	-
C_9-C_{10}-C_{11}-C_8	0.787	0.516	-0.721	-
C_9-C_{10}-C_{11}-H_{13}	-178.624	-179.011	178.7	-
C_{22}-C_{10}-C_{11}-C_8	-179.405	-179.499	179.7	-
C_{22}-C_{10}-C_{11}-H_{13}	1.185	0.974	-0.777	-
C_9-C_{10}-C_{22}-F_{23}	122.640	122.584	-119.8	-
C_9-C_{10}-C_{22}-F_{24}	1.812	1.791	-0.814	-
C_9-C_{10}-C_{22}-F_{25}	-118.865	-118.861	118.3	-
C_{11}-C_{10}-C_{22}-F_{23}	-57.168	-57.401	60.38	-
C_{11}-C_{10}-C_{22}-F_{24}	-177.996	-178.194	179.4	-
C_{11}-C_{10}-C_{22}-F_{25}	61.327	61.154	-61.38	-

Some dihedral angles between the benzene ring and the pyridine ring can be given as follows:

C_2–C_3–C_4–C_9 : –178.783 / –179.04 (cc-pVDZ / 6-311G(d,p)),

C_2–C_3–C_8–C_{11} : 179.085 / 179.206 (cc-pVDZ / 6-311G(d,p)),

C_8–C_3–C_4–N_{14} : –177.888 / –178.565 (cc-pVDZ / 6-311G(d,p)),

N_{14}–C_4–C_9–C_{10} : 178.908 / 179.239 (cc-pVDZ / 6-311G(d,p)).

These results are also in agreement with the reference molecule studies [19,30].

4.2. Vibrational assignments

Since the title molecule has 25 atoms, it has 69 vibrations. This molecule has C_s symmetry. For this reason, this molecule has in-plane 53 and out-of-plane 16 vibrational modes.

Normal modes of vibration, scaled vibration frequencies, IR & Raman vibration frequencies and intensities are given in **Table 2.** Experimental values in FT-IR and Raman spectra are also given in the same table. The experimentally measured and theoretically calculated Infrared and Raman spectra of the title molecule are given in **Figure 2, 3, 4, 5, 6 and 7**, respectively.

The crude values of the vibration frequencies obtained from the Gaussian09 program are higher than the experimental values. Due to the natural approximations and negligence of quantum mechanical methods, these calculated frequency values were multiplied by the relevant scale factors and written in **Table 2.** These scale factors can be given as follows for the basis sets used: 0.970 for the cc-pVDZ basis set, 0.966 for the 6-311G(d,p) basis set [31]

The calculated and scaled frequency values are quite compatible with the experimental values observed. Let's examine some fundamental vibrations of the AM7TFMQ molecule separately.

Table 2. Vibrational assignments of the **4-amino-2-methyl-7(trifluoromethyl)quinoline** molecule obtained as a result of the mode analysis calculated with the SQM force field.

Theoretical							Experimental		TED(%)[c]
cc-pVDZ				**6-311G(d,p)**	**cc-pVDZ[d]**	**6-311++G(d,p)[e]**	**FT-IR**	**Raman**	
Normal Modes	Freq.[a]	I_{IR}[b]	I_{Raman}[b]	Freq.[a]	Freq.	Freq.	Freq.	Freq.	
ν_1	19	0.094	0.654	14	54	15			$\tau_{CCCF}(82)+\tau_{CCCH}(9)$
ν_2	65	0.334	1.362	32	59				$\tau_{CCCH}(32)+\tau_{CCHN}(23)+\tau_{CCCC}(20)+\tau_{CCCN}(10)$
ν_3	73	0.150	0.067	65	67				$\tau_{CCCH}(40)+\tau_{CCHN}(38)$
ν_4	109	0.131	0.590	103	129	103			$\gamma_{CCCH}(24)+\gamma_{CCHN}(18)+\gamma_{CCCN}(16)+\gamma_{CCCF}(14)+\gamma_{CCCC}(13)$
ν_5	127	0.133	0.115	127	132			148 vs	$\delta_{CCC}(24)+\tau_{CCCH}(10)+\tau_{CCCN}(9)$
ν_6	178	1.495	0.424	175	168	155			$\gamma_{CCCC}(27)+\gamma_{CCCN}(25)+\gamma_{CCCH}(19)+\tau_{CCCF}(10)$
ν_7	190	0.213	0.220	188	184	186			$\gamma_{CCCC}(30)+\gamma_{CCCN}(23)+\gamma_{CCCH}(18)+\gamma_{CCCF}(9)$
ν_8	245	1.144	2.199	245	260	267		214 vs	$\delta_{CCC}(18)+\tau_{CCNH}(18)+\nu_{CC}(12)+\delta_{CCN}(10)$
ν_9	258	0.337	0.508	258	276			267 vs	$\delta_{CCC}(21)+\tau_{CCNH}(17)+\delta_{CCN}(12)$
ν_{10}	298	1.269	0.075	292	285	300			$\gamma_{CCCC}(21)+\gamma_{CCCH}(21)+\gamma_{CCCN}(20)+\gamma_{CCNH}(20)$
ν_{11}	309	0.550	0.625	310	309	302			$\tau_{CCNH}(23)+\delta_{CCN}(13)+\delta_{CCC}(10)+\tau_{CCCC}(10)$
ν_{12}	337	8.486	0.488	330	330				$\gamma_{CCNH}(46)+\tau_{CCCC}(15)+\gamma_{CCCH}(11)$
ν_{13}	357	3.911	0.077	354	357	347			$\gamma_{CCCC}(29)+\gamma_{CCCH}(20)+\gamma_{CCNH}(19)+\gamma_{CCCN}(13)$
ν_{14}	396	1.094	0.114	395	370				$\delta_{CCC}(16)+\tau_{CCNH}(16)+\delta_{CCF}(11)+\delta_{FCF}(11)+\delta_{CCN}(10)$
ν_{15}	441	0.762	2.279	440	453	434		453 s	$\tau_{CCCC}(18)+\delta_{CCC}(16)+\tau_{CCCH}(13)+\delta_{CCN}(9)+\tau_{CCNH}(9)$
ν_{16}	448	5.530	0.669	441	478	447		456 s	$\gamma_{CCCC}(29)+\gamma_{CCCH}(21)+\gamma_{CCCN}(12)+\gamma_{CCNH}(10)$
ν_{17}	505	4.545	0.554	469	495	500			$\delta_{CCC}(13)+\delta_{CCN}(18)+\gamma_{CCNH}(13)+\delta_{CCH}(9)$
ν_{18}	513	3.232	0.213	505	524	505			$\tau_{CCCC}(23)+\tau_{CCCH}(18)+\tau_{CCCN}(17)+\tau_{CCNH}(11)+\tau_{CCCF}(9)$
ν_{19}	527	52.649	1.562	511	528	526		518 m	$\gamma_{CCNH}(34)+\gamma_{CCCC}(11)+\gamma_{CCCH}(9)$
ν_{20}	543	23.382	2.827	538	535	535		523 m	$\tau_{CCNH}(25)+\delta_{CCC}(11)+\tau_{CCCC}(9)$
ν_{21}	565	0.770	0.231	561	546	554	562 w	561 s	$\delta_{CCC}(21)+\tau_{CCCF}(14)+\delta_{CCN}(13)+\delta_{CCH}(9)$
ν_{22}	587	2.928	0.737	585	584		585 m	600 m	$\delta_{CCC}(23)+\delta_{CCH}(14)+\nu_{CC}(12)$
ν_{23}	602	1.537	0.415	593	590		601 m	604 m	$\gamma_{CCCN}(24)+\gamma_{CCCH}(23)+\gamma_{CCCC}(16)+\gamma_{CCHN}(10)$
ν_{24}	635	8.695	0.555	619	625	627			$\gamma_{CCCC}(26)+\gamma_{CCCH}(22)+\gamma_{CCCN}(20)$
ν_{25}	665	2.774	3.360	661	667	652			$\delta_{CCC}(19)+\tau_{CCNH}(14)+\tau_{CCCC}(11)+\nu_{CC}(10)$
ν_{26}	674	1.545	0.023	669	692	655	681 m	676 m	$\gamma_{CCCN}(24)+\gamma_{CCCH}(21)+\gamma_{CCCC}(20)+\gamma_{CCCF}(16)$
ν_{27}	712	1.888	0.776	707	715	750	733 m	731 m	$\delta_{CCC}(19)+\nu_{CC}(16)+\nu_{CF}(11)+\delta_{CCH}(10)+\delta_{CCN}(10)$
ν_{28}	758	0.365	6.078	752	755	760			$\nu_{CC}(23)+\delta_{CCC}(19)+\delta_{CCN}(13)+\delta_{CCH}(11)$
ν_{29}	771	2.150	0.620	757	818	785	775 m	735 m	$\gamma_{CCCH}(40)+\gamma_{CCCC}(21)+\gamma_{CCCN}(15)+\gamma_{CCCF}(9)$
ν_{30}	818	5.203	0.170	798	821	838	821 s		$\gamma_{CCCH}(41)+\gamma_{CCCC}(21)+\gamma_{CCCN}(17)+\gamma_{CCNH}(10)$
ν_{31}	831	4.775	0.830	828	829	863	844 w		$\gamma_{CCCH}(30)+\gamma_{CCNH}(30)+\gamma_{CCCC}(16)+\gamma_{CCCN}(12)$
ν_{32}	899	14.607	0.785	895	861	874	862 s	885 m	$\delta_{CCH}(20)+\delta_{CCC}(19)+\nu_{CC}(10)+\tau_{CCCH}(10)$
ν_{33}	921	4.829	0.385	901	915		900 m		$\gamma_{CCCH}(41)+\gamma_{CCCC}(21)$
ν_{34}	932	1.784	0.194	929	962	948	919 m	924 m	$\tau_{CCCH}(52)+\tau_{CCCC}(14)+\tau_{CCNH}(13)$

ν_{35}	958	0.213	0.210	956	967	977			$\delta_{CCH}(23)+\delta_{CCC}(15)+\nu_{CC}(13)+\delta_{CCN}(11)+\tau_{CCCH}(9)$
ν_{36}	987	8.811	1.542	985	981	985	1010 m	981 m	$\delta_{CCH}(25)+\delta_{CCC}(16)+\nu_{CC}(11)$
ν_{37}	1011	0.827	0.010	1019	1012	1001			$\tau_{CCCH}(28)+\delta_{CCH}(20)+\gamma_{CCCN}(18)+\tau_{CCNH}(11)$
ν_{38}	1041	13.818	1.505	1037	1057	1037	1067 s		$\delta_{CCH}(32)+\nu_{CC}(19)+\nu_{CF}(10)$
ν_{39}	1059	3.709	0.284	1049	1065	1043		1066 m	$\delta_{CCH}(23)+\delta_{CCC}(17)+\delta_{CNH}(15)+\nu_{CC}(12)$
ν_{40}	1105	5.330	1.794	1062	1097	1074		1070 m	$\delta_{CCH}(26)+\nu_{CC}(17)+\delta_{CCC}(15)$
ν_{41}	1121	88.002	1.014	1097	1130	1125	1117 vs		$\tau_{CCCF}(24)+\nu_{CF}(21)+\tau_{CCCH}(16)+\tau_{CCCC}(13)+\delta_{CCF}(9)+\delta_{FCF}(9)$
ν_{42}	1141	20.483	1.618	1106	1149	1140	1150 s		$\delta_{CCH}(27)+\nu_{CC}(16)+\nu_{CF}(10)$
ν_{43}	1158	59.691	1.445	1147	1155	1180	1176 s	1159 m	$\delta_{CCH}(24)+\nu_{CF}(17)+\tau_{CCCF}(13)+\nu_{CC}(11)$
ν_{44}	1168	0.943	1.363	1171	1163	1198		1197 m	$\delta_{CCH}(39)+\nu_{CC}(14)+\delta_{CCC}(11)$
ν_{45}	1217	32.795	0.188	1213	1202		1237 m	1259 m	$\delta_{CCH}(38)+\delta_{CCC}(12)+\nu_{CC}(10)$
ν_{46}	1227	5.300	0.046	1230	1256	1252	1264 w	1267 m	$\delta_{CCH}(37)+\nu_{CC}(13)+\delta_{CCC}(10)+\nu_{CN}(9)$
ν_{47}	1292	100	2.737	1271	1281	1287	1311 vs		$\nu_{CC}(26)+\delta_{CCH}(18)+\delta_{CCC}(11)$
ν_{48}	1331	6.668	2.975	1323	1328		1343 w	1344 m	$\delta_{CCH}(28)+\nu_{CC}(17)+\delta_{CCC}(10)+\delta_{CNH}(10)$
ν_{49}	1340	0.022	2.560	1346	1338	1358			$\delta_{CCH}(35)+\delta_{HCH}(18)+\nu_{CC}(15)$
ν_{50}	1371	13.853	63.276	1350	1360	1372			$\nu_{CC}(34)+\delta_{CCH}(22)+\delta_{CCC}(10)$
ν_{51}	1383	12.587	7.220	1371	1383	1381	1374 s	1375 m	$\nu_{CC}(16)+\delta_{HCH}(16)+\delta_{CCH}(12)+\delta_{CCN}(10)+\tau_{CCCN}(9)+\tau_{CCNH}(9)+\delta_{CCC}(9)$
ν_{52}	1397	10.863	15.899	1405	1401	1402			$\delta_{HCH}(20)+\delta_{CCH}(13)+\nu_{CC}(12)+\tau_{CCNH}(12)+\tau_{CCNH}(11)+\delta_{CCC}(9)$
ν_{53}	1411	2.030	5.924	1431	1411	1445	1427 w		$\delta_{HCH}(34)+\tau_{CCCH}(24)+\tau_{CCNH}(24)+\delta_{CCH}(9)$
ν_{54}	1437	1.148	14.705	1435	1421	1463			$\delta_{CCH}(26)+\nu_{CC}(19)+\delta_{CCC}(13)$
ν_{55}	1443	6.704	15.978	1440	1462	1470	1454 w	1460 m	$\delta_{CCH}(30)+\nu_{CC}(20)+\delta_{CCC}(12)+\delta_{HCH}(9)$
ν_{56}	1511	27.278	1.313	1497	1510	1485	1523 s	1560 m	$\delta_{CCH}(32)+\nu_{CC}(28)+\delta_{CCC}(13)$
ν_{57}	1561	14.033	6.786	1542	1571	1531	1563 m	1563 m	$\nu_{CC}(25)+\delta_{CCC}(18)+\delta_{CCH}(17)+\delta_{CCN}(11)$
ν_{58}	1585	24.698	3.441	1580	1584	1581	1596 s	1593 m	$\tau_{CCNH}(16)+\nu_{CC}(15)+\delta_{HNH}(14)+\delta_{CCH}(13)+\delta_{CCC}(10)$
ν_{59}	1614	77.563	10.031	1609	1609	1616	1627 m	1621 m	$\nu_{CC}(18)+\delta_{CCH}(15)+\delta_{CCC}(14)+\tau_{CCNH}(13)+\delta_{HNH}(11)+\delta_{CNH}(9)$
ν_{60}	1629	0.361	6.262	1613	1619	1638	1650 m	1629 m	$\nu_{CC}(33)+\delta_{CCH}(28)+\delta_{CCC}(19)$
ν_{61}	2939	7.238	100	2924	2939	2903	2924 w	2925 m	$\nu_{CH}(89)$
ν_{62}	2995	4.793	42.457	2970	2996	2949		2983 w	$\nu_{CH}(77)$
ν_{63}	3055	1.918	23.281	3029	3057	3035	3034 w	3037 m,sh	$\nu_{CH}(77)$
ν_{64}	3072	5.484	46.147	3052	3072	3043	3055w	3060 m	$\nu_{CH}(72)$
ν_{65}	3086	2.686	17.567	3064	3084	3059	3069 w	3072 m	$\nu_{CH}(76)$
ν_{66}	3112	2.043	54.920	3089	3104	3068	3101 w	3095 m,sh	$\nu_{CH}(79)$
ν_{67}	3131	0.048	26.035	3107	3128			3138 w	$\nu_{CH}(75)+\delta_{CCC}(10)$
ν_{68}	3444	7.634	67.706	3469	3443	3442	3407 w	3407 vw	$\nu_{NH}(87)$
ν_{69}	3542	5.582	20.874	3566	3541	3538	3469 w	3508 vw	$\nu_{NH}(84)$

ν: stretching, τ: torsion, γ: out of plane stretching, δ: in plane bending vs: very strong, ms: medium strong, s: strong, w: weak, vw: very weak,

[a] Scaled with a value of 0.970 for the cc-pVDZ basis set and 0.965 for the 6-311 basis set. [b] Infrared and Raman intensities were calculated by normalizing the highest intensity value to 100.

[c] Total energy distributions calculated with the B3LYP/6-311G(d,p) basis set. Only contributions≥ 9 % are listed.

[d] Sertbakan T R, Celal Bayar University Journal of Science, 13(4) (2017) 851. [Ref. 19] [e] Arjunan V, Saravanan I, Ravindran P, Mohan S, Spectrochim Acta, A74/2 (2009) 375. [Ref. 30]

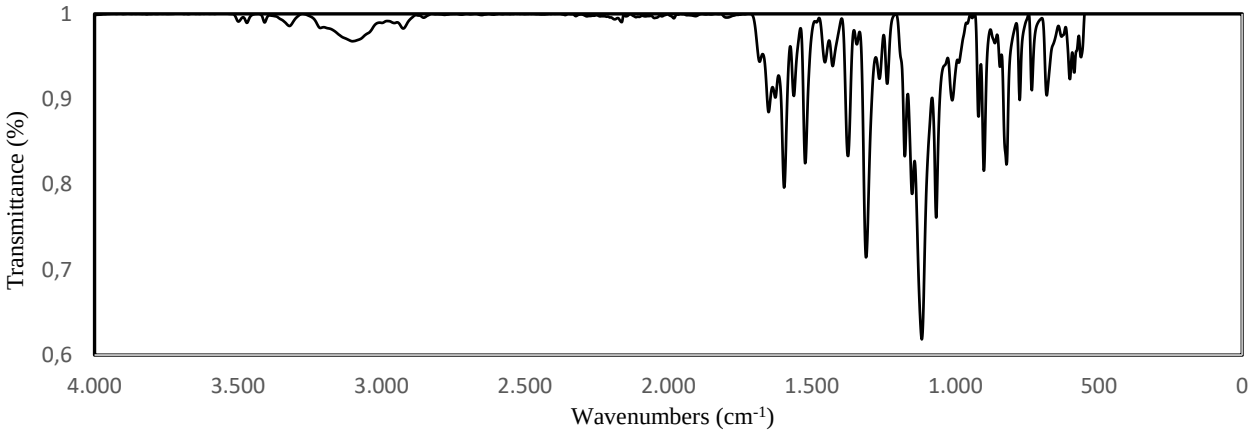

Figure 2. The experimental FT-IR spectrum of 4-amino-2-methyl-7(trifluoromethyl) quinoline

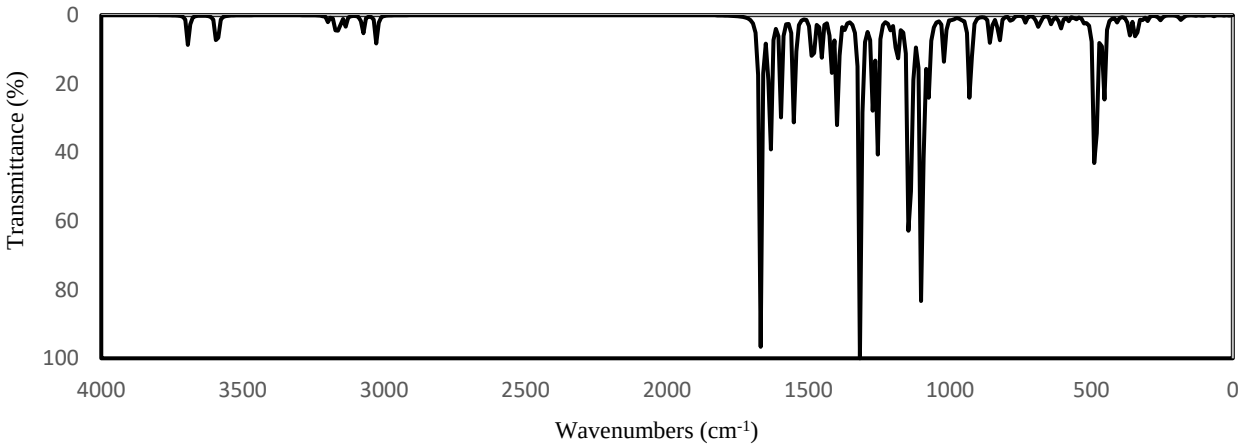

Figure 3. Theoretical IR spectrum of the 4-amino-2-methyl-7(trifluoromethyl)quinoline molecule calculated with the 6-311G(d,p) basis set

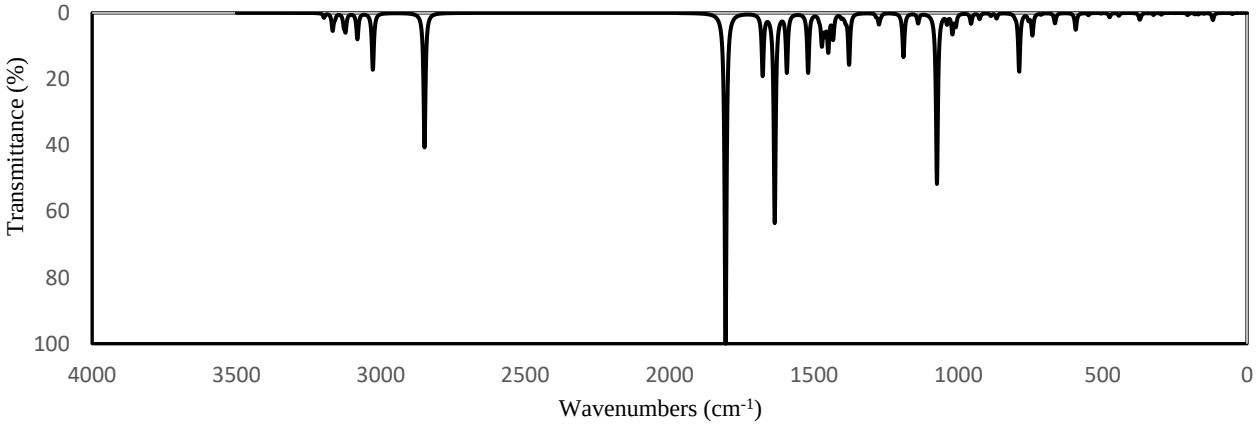

Figure 4. Theoretical IR spectrum of the 4-amino-2-methyl-7(trifluoromethyl)quinoline molecule calculated with the cc-PVDZ basis set

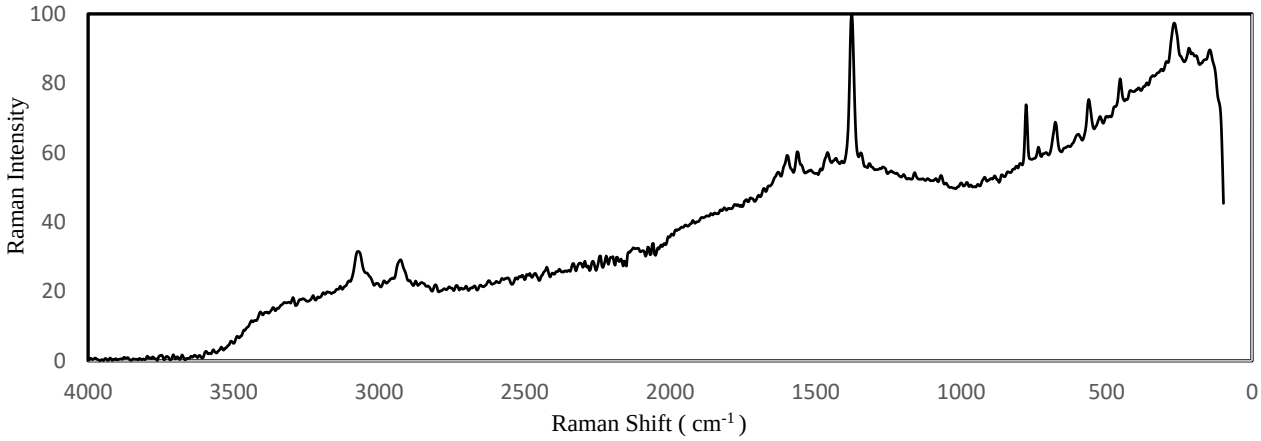

Figure 5. The experimental Raman spectrum of 4-amino-2-methyl-7(trifluoromethyl)quinolone

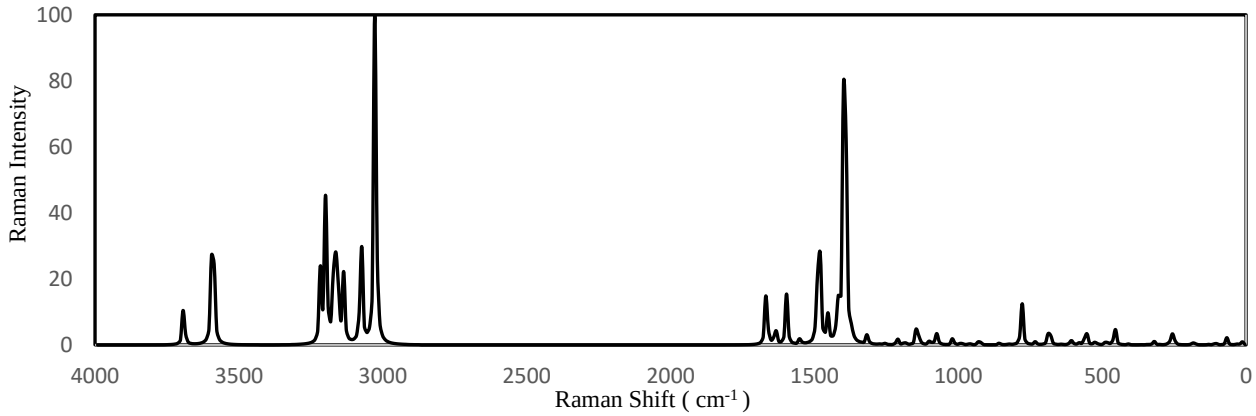

Figure 6. Theoretical Raman spectrum of the 4-amino-2-methyl-7(trifluoromethyl)quinoline molecule calculated with the 6-311G(d,p) basis set

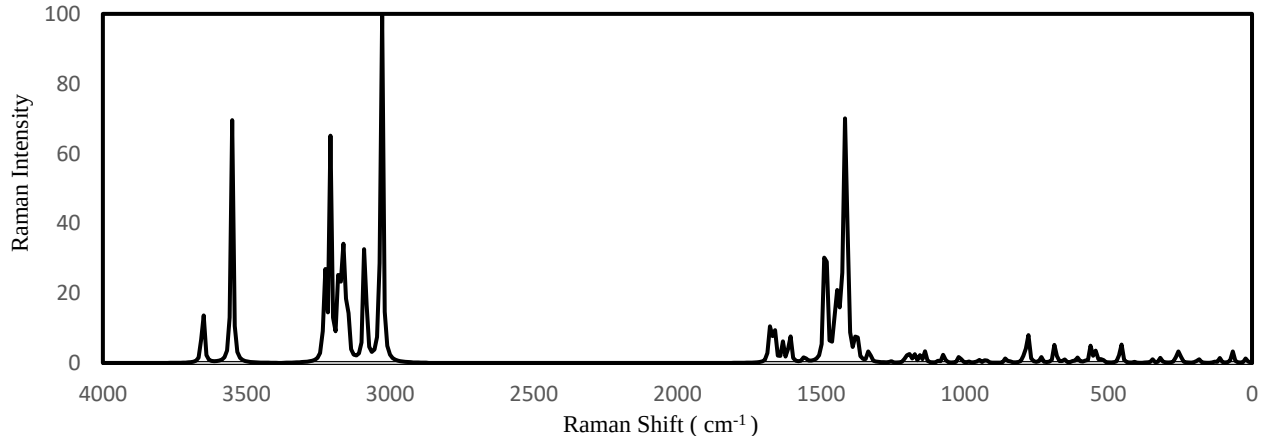

Figure 7. Theoretical Raman spectrum of the 4-amino-2-methyl-7(trifluoromethyl)quinoline molecule calculated with the cc-PVDZ basis set

4.2.1. C–C vibrations

Ring C–C stretching vibrations have characteristic features for aromatic rings. These C–C stretching vibration modes were observed in the region of 1430–1625 cm^{-1} for the phenyl group [32]. These vibrations were observed at 1650, 1627, 1563, 1427 cm^{-1} in the experimental FT-IR spectrum and 1629, 1621, 1563, cm^{-1} in the experimental Raman spectrum. Theoretically, C–C stretching vibration frequencies calculated with the DFT/B3LYP method cc-PVDZ basis set can be given as 1629, 1614, 1561, 1411 cm^{-1}.

In-plane C–C–C bending vibrational frequencies were always observed at 1000–600 cm^{-1} region [33]. The experimentally observed frequency values of this vibration mode are in the range of 862–585 cm^{-1}. Theoretically, these frequency values were calculated between 899 and 587 cm^{-1} in cc-pVDZ basis set. It can be seen that the experimental and theoretical results are consistent when the frequencies of vibrations in this region are examined one by one.

4.2.2. C–H vibrations

Aromatic C–H stretching vibration frequencies were observed in the range of 3100–3000 cm^{-1} [34]. All of the C–H stretching vibration frequencies in the spectra were observed as weak intensity peaks. This is because the negative charge around the carbon atom and the dipole moment of this bond decreases [35]. This decrease is the result of the decrease in the inductive effect caused by the electron withdrawal from the carbon atom of the molecule. In this case, there is an increase in the bond length of the molecule. [36]. These vibrational frequencies of our molecule were observed at 3101, 3069, 3055, 3034 cm^{-1} in the experimental FT-IR spectrum. The same vibration frequencies were observed at 3095, 3072, 3060, 3037 in the Raman spectrum and these frequencies were marked as C–H in-plane bending vibration frequencies. **Table 2** shows that the experimental and theoretical results of the mentioned frequencies are compatible.

C–C–H in-plane bending vibration frequencies are characterized in the region of 1300–1000 cm^{-1} [37]. The in-plane bending vibration frequencies C–C–H of the title molecule were measured at 1523, 1454, 1343, 1311, 1264, 1237 cm^{-1} (in the FT- IR spectrum) and at 1560, 1460, 1344, 1267, 1259 cm^{-1} (in the Raman spectrum). The frequencies of this vibration calculated with the cc-PVDZ basis set in the (DFT)/B3LYP method are 1511, 1443, 1331, 1292, 1227 and 1217 cm^{-1}.

The frequencies of the out-of-plane C–C–H angle bending vibration are in the region of 1000–750 cm^{-1} in the literature [38]. The frequencies of this vibration were observed at 844, 821, 775 cm^{-1} in the IR spectrum and 885, 735 cm^{-1} in the Raman spectrum. As a result of theoretical calculations (DFT/B3LYP method, cc-PVDZ basis set), these vibrational frequencies were found as 831, 818, 771 cm^{-1}.

Finally, while the asymmetric CH_3 stretching vibration in the methyl group was observed at 1411 cm^{-1} in the FT-IR spectrum, the theoretical result for this vibration was calculated to be 1427 cm^{-1}.

All these in-plane and out-of-plane C - C - H bending vibration frequencies were found to be consistent with the studies in the literature [19, 30].

4.2.3. N–H vibrations

N–H stretching vibration frequencies are in the range of 3500 – 3350 cm^{-1} [39]. In our study, N–H stretching vibration frequency values were observed experimentally at 3469 / 3508 cm^{-1} (FT-IR/Raman) and 3407 / 3407 cm^{-1} (FT-IR/Raman). As a result of the theoretical calculations made with the DFT / B3LYP method and the cc-PVDZ basis set, these frequencies were fund to be 3542 and 3444 cm^{-1}. As **Table 2** shows, TED results for these vibrations are close to 90%.

N–H deformation vibration frequencies were experimentally reported as 1538 / 1538 cm^{-1} (FT-IR / Raman) and 1220 / 1223 cm^{-1} (FT-IR / Raman) [40]. In our spectrum, I observed frequencies of this vibration at 1596 / 1593 and – / 1066 cm^{-1} (FT-IR/Raman). In my calculations, I found these frequencies as 1585 and 1059 cm^{-1}.

4.2.4. C–N vibrations

In our molecule, the bond between the carbon atom and the nitrogen atom is the singular and double states. Hence, it is difficult to distinguish the vibration frequencies associated with these two bonds in the C–N region of the spectrum. The C=N and C–N stretching vibrations were observed at 1689 and 1302 cm^{-1}, respectively, in the FT-IR spectrum [41].

In my work, I also used TED results and assignment the frequencies I observed in my spectra at 1374/1375 cm^{-1} (IR/Raman) as C–N (single bond) stretching vibrations. In my theoretical calculations, this frequency is 1383 cm^{-1}.

4.2.5. C–F vibrations

The bands I observed at frequencies of 1176, 1150 and 1117 cm^{-1} (FT-IR) were assignment as C–F stretching vibrations with the help of TED results. Theoretical calculation results for these frequency values are 1158, 1141 and 1121 cm^{-1}.

The experimental and theoretically calculated FT-IR and Raman spectra of the AM7TFMQ molecule are given in **Table 2**.

In addition, all these vibrations that I have calculated and given above are in agreement with the vibration frequencies in the two studies I reference, as seen in **Table 2** [19,30].

4.3. NMR Analysis

The chemical shift is used as an aid to spectral marking and structural identification. Significant progress has been made in calculations in this area. Isotropic chemical shifts often help to accurately predict the geometry of molecules and identify organic compounds. The DFT-B3LYP [21] and DFT-B3PW91 [42] calculations are in good agreement with GIAO approach, which uses density theory with experimental NMR spectrum analysis. Therefore, I performed my NMR calculations in DMSO (dimethylsulfoxide) solution using the DFT/B3LYP method, cc-pVDZ and 6-311G (d,p) basis sets. The ^{13}C NMR nuclear shielding constant was estimated by the GIAO approach. Calculated ^{1}H and ^{13}C absolute isotropic shielding parameters were converted to ^{1}H and ^{13}C chemical shifts.

The experimental peaks in ^{1}H and ^{13}C NMR spectra of the 4-amino-2-methyl-7(trifluoromethyl) quinoline molecule are shown in **Figure 8** and **Figure 9**. The NMR (^{1}H and ^{13}C) experimental and theoretical chemical shifts of my molecule in DMSO solution are given in **Table 3**.

The signal at 159.82 ppm, the value for the fifth carbon in the NMR spectrum, was observed. This signal was obtained as 166.09 ppm for the cc-pVDZ basis set and 172.34 ppm for the 6-311G(d,p) basis set in our theoretical calculations. The experimental signal for carbon (C_2) in the amino group is 152.86 ppm, while theoretically this signal is calculated as 155.33 ppm and 163.14 ppm, respectively, for the basis sets given above.

The NMR spectrum was taken to measure the different effects that may occur on the chemical shift of the proton. The proton chemical shifts observed in this region are in the range of 8.375 – 2.508 ppm In the NMR spectrum of the proton, chemical shifts for the hydrogens in the quinoline ring (H_7, H_6, H_{12} and H_{13}) were observed at 7.63, 8.37, 8.34 and 7.99 ppm, respectively.

For the hydrogen atoms in the methyl group (H_{19}, H_{20} and H_{21}), these shifts were observed at 2.51, 2.71 and 2.51 ppm. The chemical shifts for hydrogens bound to nitrogen are 2.675 and 2.853 ppm.

The results for the theoretical and experimental chemical shifts I obtained in the NMR spectra of my molecule are shown in **Table 3**. I also compared the NMR spectrum results related to my molecule with my previous reference study and found it to be compatible (Table 1). The result of this comparison showed some minor differences. It can be thought that the reason for these differences is where the CF_3 group is attached.

Table 3. Theoretical and experimental ^{1}H and ^{13}C NMR spectral data of 4-amino-2-methyl-7(trifluoromethyl) quinoline molecule (ppm - in DMSO solution)

	B3LYP (Theoretical)		Experimental	Ref. [19]
	cc-pVDZ	6-311G(d,p)		cc-pVDZ
6-H	8.7263	8.9984	8.3746	7.849
12-H	7.8862	8.2346	8.3458	7.430
13-H	7.6360	7.8879	7.9915	8.028
7-H	7.1358	7.4189	7.6286	6.474
17-H	2.6608	2.9323	2.8532	3.385
20-H	2.2058	2.3561	2.7110	2.817
16-H	2.1176	2.3370	2.6754	3.954
19-H	1.9795	2.1417	2.5139	2.825
21-H	1.8281	2.0161	2.5080	2.651
	B3LYP (Theoretical)		Experimental	Ref. [19]
	cc-pVDZ	6-311G(d,p)		cc-pVDZ
5-C	166.0916	172.3379	159.8183	161.9
2-C	155.3291	163.1420	152.8580	149.4
10-C	142.4369	147.6123	–	129.1
4-C	142.2926	148.1621	146.7271	148.3
22-C	131.7089	135.9210	130.2614	131.4
8-C	130.1454	135.9732	129.8406	124.5
9-C	125.0944	131.2319	129.4193	134.4
1-C	123.6075	128.1638	125.9324	105.4
11-C	123.2227	129.0398	126.3699	123.4
3-C	122.6908	127.0622	124.8797	121.5
18-C	24.4636	25.8265	24.5174	29.1

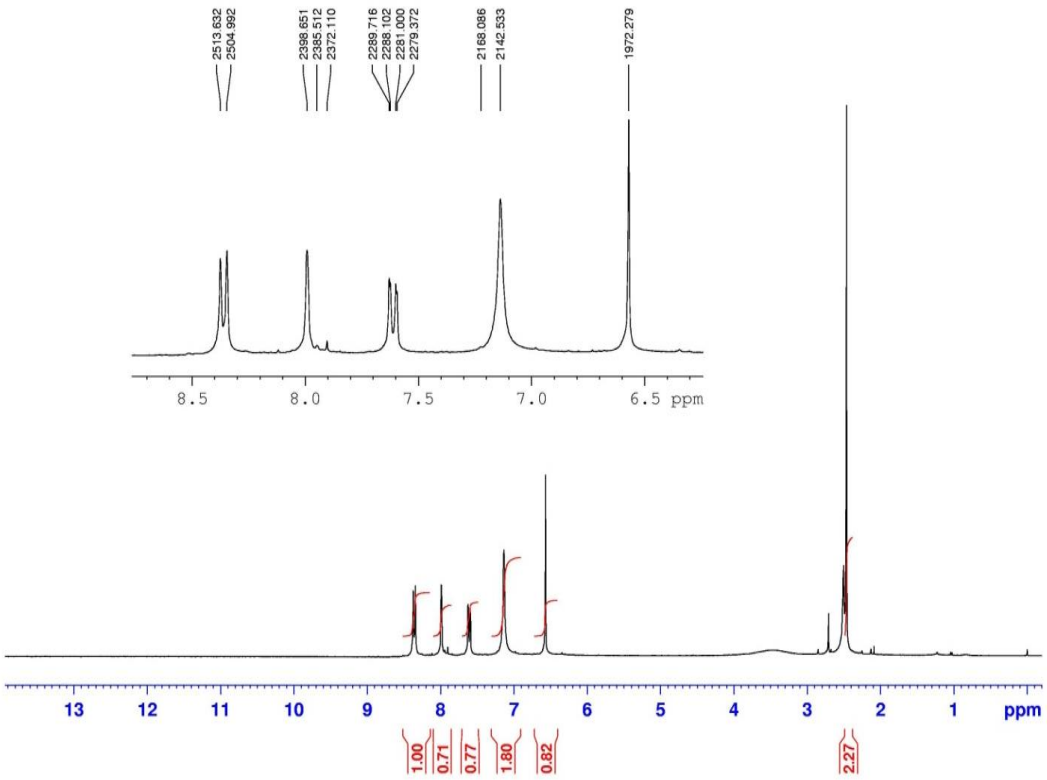

Figure 8. The ^{1}H NMR spectra of 4-amino-2-methyl-7(trifluoromethyl)quinoline molecule.

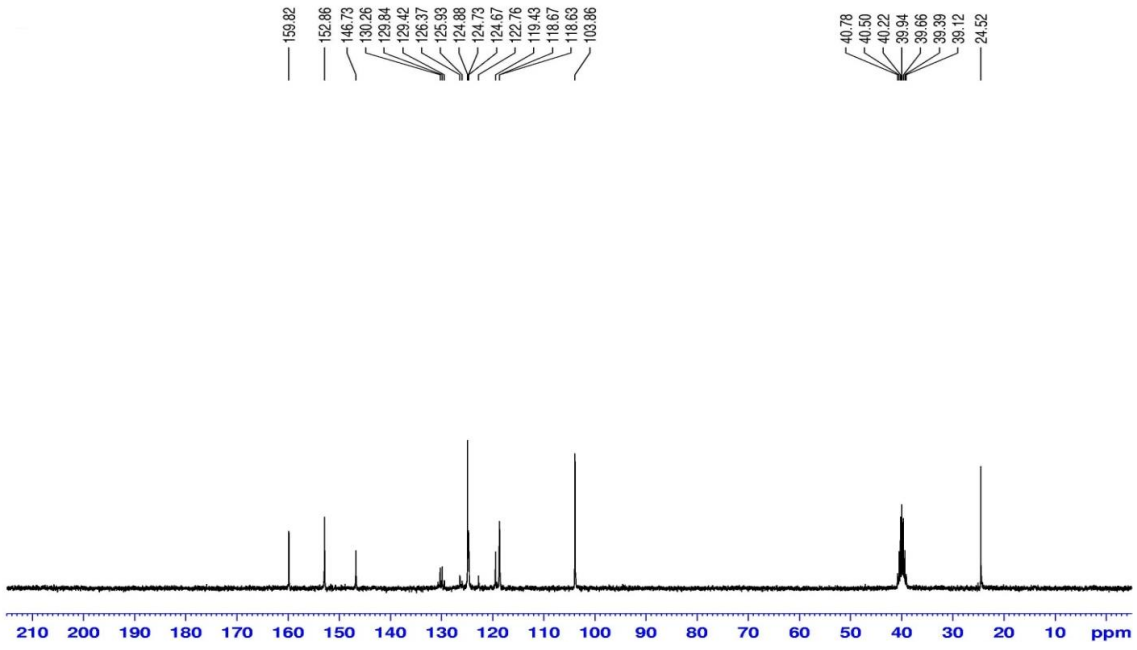

Figure 9. The ^{13}C NMR spectra of 4-amino-2-methyl-7(trifluoromethyl)quinoline molecule.

4.4. HOMO - LUMO analysis

They are known as the HOMO (highest occupied molecular orbital), the LUMO (lowest unoccupied molecular orbital) molecular orbitals and have important place in the Quantum Chemistry. The LUMO can be regarded as the innermost orbital for placing electrons. The HOMO is the outermost molecular orbital that can be filled with electrons. The HOMO characterizes the ability to give electrons. An excited electron makes an electronic transition from the HOMO orbital to the LUMO boundary molecular orbital. This absorption is from the ground electronic level to the first excited electronic level. These boundary molecular orbital energies known for chemical compounds are important parameters for quantum mechanics.

The bioactivity and chemical activity of the molecule, which is one of the important features of a molecule, is related to the eigenvalues of $\Delta E_{HOMO-LUMO}$ energy gap and HOMO, LUMO energy levels. $\Delta E_{HOMO-LUMO}$ energy range is in the range of 3 eV. This value helps us explain the interacting charge transfer in a molecule. The lower this value, the less stable the molecule [43].

In addition, these molecular orbitals play important roles in electrical – optical properties, chemical reactions, and UV visible spectra [44].

The HOMO, HOMO-1 and LUMO, LUMO+1 molecular orbitals drawn by Gaussian09 of the 4-amino-2-methyl-7(trifluoromethyl) quinoline molecule are given in **Figure 10.** The energy values of these levels can also be seen in this figure.

4.5. Molecular Electrostatic Potential (MEP) maps

The Molecular Electrostatic Potential (MEP) maps of the AM7TFMQ molecule given in **Figure 11** are quite stable. The MEP maps can often be seen as a map of reactivity where the most probable regions of point charges on organic molecules can approach molecular. In addition, the MEP maps help to predict how structures with different geometries interact [19].

In the calculated three-dimensional MEP map, the red regions are negatively charged and the blue regions are positively charged. The positive regions are the regions where the nitrogen and fluorine atoms are located. It is easier for other chemical structures to interact with the positive regions of any molecule. In this case, the title molecule interacts with the nitrogen and fluorine atoms.

5. Conclusions

In the current study, quantum chemical calculations of the 4-amino-2-methyl-7(trifluoromethyl) quinoline molecule were carried out using the density function theory (DFT), with the Gaussian 09 software package, cc-pVDZ and 6-311G(d,p) basis sets at the B3LYP level. All these calculations were made in the gas phase. The geometric parameters of the title molecule were calculated using the same method and basis sets. The vibration frequencies of the molecule were calculated experimentally and theoretically by Infrared and Raman Spectroscopy methods. These calculations were compared with experimental results. In addition, the NMR spectrum of the molecule was calculated using the same method and basis sets. It has been observed that all these experimental observations and calculated values are quite compatible. In addition, these values were compared with the values in the reference studies and the results were again compatible. HOMO-LUMO molecular orbital levels and $\Delta E_{HOMO-LUMO}$ energy gap of our molecule were also calculated using the above methods. It was observed that the data obtained as a result of these calculations are in agreement with previous studies on the subject. Finally, MEP maps of the molecule were drawn. In this way, the most likely regions of the molecule to bond are determined.

Acknowledgements

I would like to thank the Kırşehir Ahi Evran University Scientific Research Projects unit, who assisted us in the supply of the 4-amino-2-methyl-7(trifluoromethyl) quinoline molecule I used in this study.

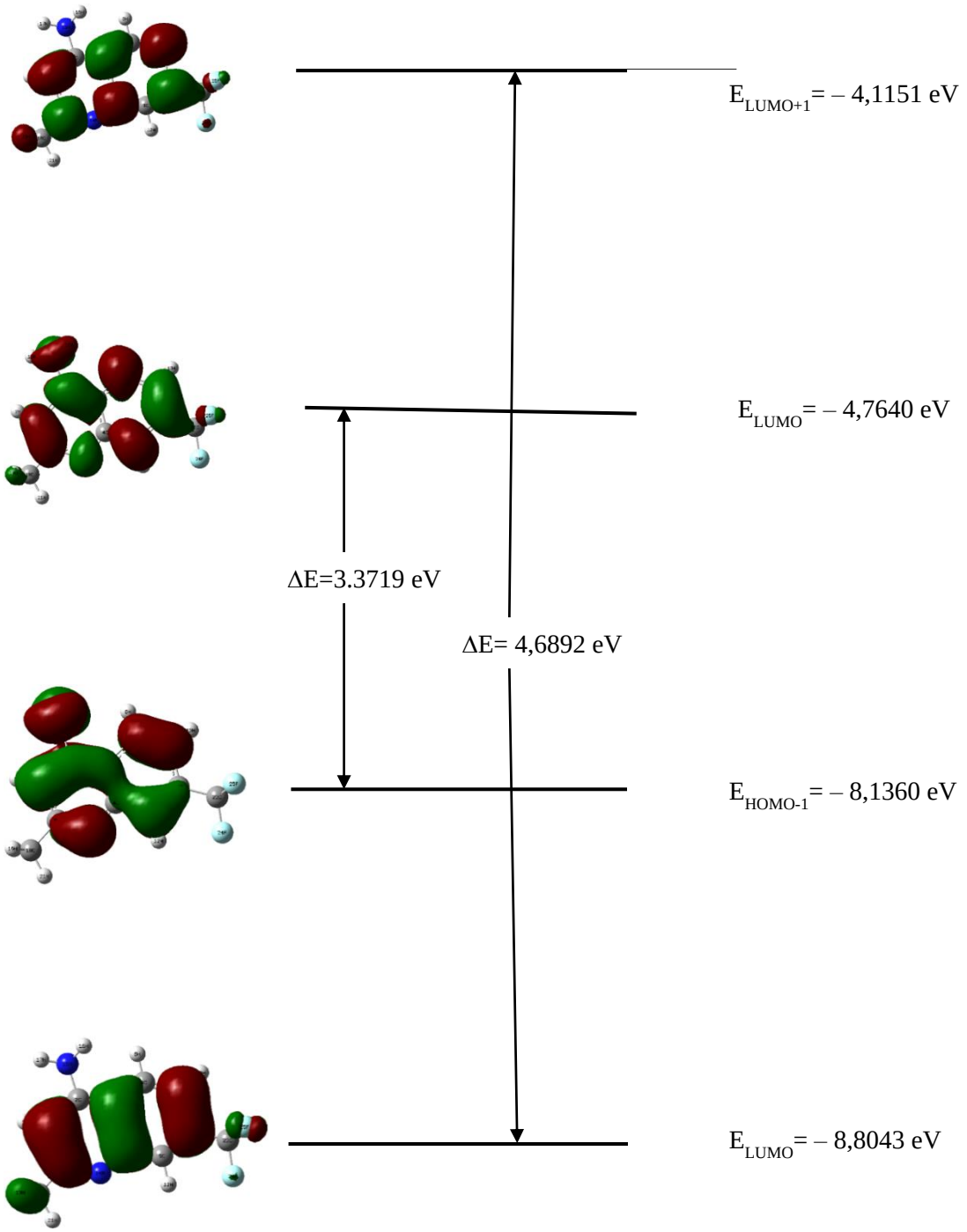

Figure 10. Atomic compositions of the boundary molecule orbital for the 4-amino-2-methyl-7(trifluoromethyl) quinoline molecule

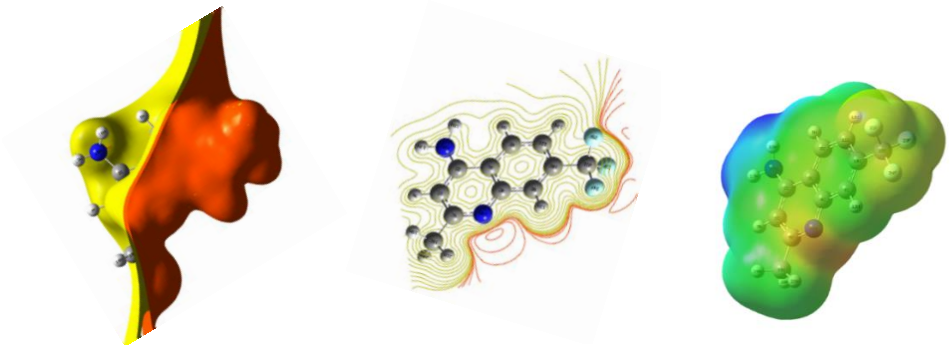

Figure 11. MEP maps calculated for the 4-amino-2-methyl-7(trifluoromethyl)quinoline molecule at the B3LYP/6-31G (d,p)

References

[1] Eswaran S, Adhikari AV, Shetty NS. Synthesis and antimicrobial activities of novel quinoline derivatives carrying 1,2,4-triazole moiety. Eur J Med Chem. 2009;44:4637–47.

[2] Keshk EM, El-Desoky SI, Hammouda MAA, Adbel-Rahman AH, Hegazi AG. Phosphorus Synthesis and Reactions of Some New Quinoline thiosemicarbazide derivatives of potentional biological activity. Sulfur and Silicon, 2008;183:1323–43.

[3] Kumru M, Küçük V, Kocademir M. Determination of structural and vibrational properties of 6-quinolinecarboxaldehyde using FT-IR, FT-Raman and Dispersive-Raman experimental techniques and theoretical HF and DFT (B3LYP) methods. Spectrochim Acta A. 2012;96:242–51.

[4] Kumru M, Küçük V, Kocademir M, Alfanda HM, Altun A. and Sarı L. Experimental and theoretical studies on IR, Raman, and UV–Vis spectra of quinoline-7-carboxaldehyde. Spectrochim Acta A. 2015;134:81–89.

[5] Shoair AF, El-Bindary AA, El-Sonbati AZ, Younes RM. Stereochemistry of New Nitrogen Containing Heterocyclic Aldehydes. III. Novel Bis-Bidentate Azodye Compounds. Polish J Chem. 2000;74:1047–53.

[6] Khan KM, Zaify ZS, Khan ZA, Ahmed M, Saeed M, Schick M, et al. Syntheses and Cytotoxic, Antimicrobial, Antifungal and Cardiovascular Activity of New Quinoline Derivatives. Arzneim Forsch/Drug Res. 2000;50:915–24.

[7] Deady LW, Desneres J, Kaye AJ. Positioning of the Carboxamide Side Chain in 11-Oxo-11H-indeno[1,2-b]quinolinecarboxamide Anticancer Agents: Effects on Cytotoxicity. Bioorg Med Chem. 2001; 9(2):445–52.

[8] Dube D, Blouin M, Brideau C, Chan CC, Desmarais S, Ethier D, Falgueyret JP, et al. Quinolines as potent 5-lipoxygenase inhibitors: Synthesis and biological profile of L-746,530. Bioorg Med Chem Lett. 1998;8(10):1255–60.

[9] Gupta R, Gupta AK, Paul S. Microwave-assisted synthesis and biological activities of some 7/9-substituted-4-(3-alkyl/aryl-5,6-dihydro-s-triazolo[3,4-b][1,3,4]thiadiazol-6-yl)tetrazolo[1,5-a] quinolines. Indian J Chem. 2000;39(B):847–52.

[10] Tewari S, Chauhan PM, Bhaduri AP, Fatima N, Chatterjee RK. Syntheses and antifilarial profile of 7-chloro-4-(substituted amino)quinolines : a new class of antifilarial agents. Bioorg Med Chem Lett. 2000;10(13):1409–12.

[11] Fujita M, Chiba K, Tominaga Y, Katsuhiko H. 7-(2-Aminomethyl-1-azetidinyl)-4-oxoquinoline-3-carboxylic Acids as Potent Antibacterial Agents : Design, Synthesis, and Antibacterial Activity. Chem Pharm Bull. 1998;46:787–96.

[12] Kidwai M, Bhushan KR, Sapra P, Saxena RK, Gupta R. Alumina-supported synthesis of antibacterial quinolines using microwaves. Bioorg Med Chem. 2000;8(1): 69–72.

[13] Go ML, Nigam TL, Tan ALC, Kuaha K, Wilairat P. Structure-activity relationships of some indolo[3,2-c] quinolines with antimalarial activity. Eur J Pharm Sci. 1998;6(1):19–26.

[14] Famin O, Krugliak M, Ginsburg H. Kinetics of inhibition of glutathione-mediated degradation of ferriprotoporphyrin IX by antimalarial drugs. Biochem Pharmacol. 1999;58(1):59–68.

[15] Chauhan PMS, Srivastava SK. Present Trends and Future Strategy in Chemotherapy of Malaria. Curr Med Chem. 2001;8(13):1535–42.

[16] Özel AE, Büyükmurat Y, Akyüz S. Infrared-spectra and normal-coordinate analysis of quinoline and quinoline complexes. J Mol Struct. 2001;565–566:455-62.

[17] Rosenberg E, Rokhsana D, Nervi C, Gobetto R, Milone L, Viale A, et al. Synthesis, Reduction Chemistry, and Spectroscopic and Computational Studies of Isomeric Quinoline carboxaldehyde Triosmium Clusters. Organometallics 2004;23(2):215–23.

[18] Ali MA, Mirza AH, Hamid MHSA, Bernhardt PV. Diphenyltin(IV) complexes of the 2-quinolinecarboxaldehyde Schiff bases of S-methyl- and S-benzyldithiocarbazate (Hqaldsme and Hqaldsbz): X-ray crystal structures of Hqaldsme and two conformers of its diphenyltin(IV) complex. Polyhedron. 2005;24(3):383–90.

[19] Sertbakan TR. Structure Spectroscopic and Quantum Chemical Investigations of 4-Amino-2-Methyl-8-(Trifluoromethyl)Quinoline. Celal Bayar University Journal of Science. 2017;13(4): 851–61.

[20] Pulay P, Baker J, Wolinski K. Green Acres Road Suite A Fayettevile. Arkansas 72703: USA; 2013.

[21] Ditchfield R. Molecular Orbital Theory of Magnetic Shielding and Magnetic Susceptibility. J Chem Phys. 1972;56:5688–91.

[22] Wolinski K, Hinton JF, Pulay P. Efficient implementation of the gauge-independent atomic orbital method for NMR chemical shift calculations. J Am Chem Soc. 1990;112(23):8251–60.

[23] Petersilka M, Gossmann UJ, Gross EKU. Excitation Energies from Time-Dependent Density-Functional Theory. Phys Rev Lett. 1996;76:1212–15.

[24] Karabacak M, Sinha L, Prasad O, Cinar Z, Cinar M. The spectroscopic (FT-Raman, FT-IR, UV and NMR), molecular electrostatic potential, polarizability and hyperpolarizability, NBO and HOMO–LUMO analysis of monomeric and dimeric structures of 4-chloro-3,5-dinitrobenzoic acid. Spectrocim Acta A. 2012; 93:33–46.

[25] Bauernschmitt R, Ahlrichs R, Treatment of electronic excitations within the adiabatic approximation of time dependent density functional theory. Chem Phys Lett. 1996;256(4-5):454–64.

[26] Jamorski C, Casida ME, Salahub DR. Dynamic polarizabilities and excitation spectra from a molecular implementation of time-dependent density-functional response theory: N2 as a case study. J Chem Phys. 1996;104:5134–47.
[27] Kurban M, Gündüz B, Göktaş F. Experimental and theoretical studies of the structural, electronic and optical properties of BCzVB organic material. Optik. 2019;182:611–17.
[28] Kurban M. Electronic structure, optical and structural properties of Si, Ni, B and N-doped a carbon nanotube: DFT study. Optik. 2018;172:295–301
[29] Frisch MJ, Trucks GW, Schlegel HB, Scuseria GE, Robb MA, Cheesemen JR. et al. Gaussian09 revision A2. Wallingford CT: Gaussian Inc; 2009.
[30] Arjunan V, Saravanan I, Ravindran P, Mohan S. Ab initio, density functional theory and structural studies of 4-amino-2-methylquinoline. Spectrochim Acta A. 2009;74/2:375 – 84.
[31] Merrick JP, Moran D, Radom L. An Evaluation of Harmonic Vibrational Frequency Scale Factors. J Phys Chem A. 2007;111-45:11683–700.
[32] Varsayni G. Assignments of Vibrational spectra of Seven Hundred benzene derivatives Vol:1-2: Adamm Hilger; 1974.
[33] Fu A, Du D, Zhou Z. Density functional theory study of vibrational spectra of acridine and phenazine. Spectrochim Acta A. 2003;59(2):245–53.
[34] Karabacak M, Kurt M, Ataç A. Experimental and theoretical FT-IR and FT-Raman spectroscopic analysis of N1-methyl-2-chloroaniline. J Phys Org Chem. 2009;22(4):312–30.
[35] Sas EB, Kurt M, Karabacak M, Poiyamozdi A, Sundaraganesan N. FT-IR, FT-Raman, dispersive Raman, NMR spectroscopic studies and NBO analysis of 2-Bromo-1H-Benzimidazol by density functional method. J Mol Struct. 2015;1081:506-18.
[36] Sundaraganesan N, Saleem H, Mohan S. Vibrational spectra, assignments and normal coordinate analysis of 3-aminobenzyl alcohol. Spectrochim Acta A. 2003;59: 2511–17.
[37] Thilagavathi G, Arivazhagan M. Density functional theory calculation and vibrational spectroscopy study of 2-amino-4,6-dimethyl pyrimidine (ADMP). Spectrochim Acta A. 2011; 79: 389–95
[38] Shanmugam R, Sathyanarayana D. Experimental (FT-IR and FT-Raman), electronic structure and DFT studies on 1-methoxynaphthalene. Spectrochim Acta A. 1984;40:757–61.
[39] Spire A, Barthes M, Kellouai H, De Nunzio G. Far-infrared spectra of acetanilide revisited. Physics D. 2000;137:392–401.
[40] Panicker CY, Varghese HT, Thansani T. Spectroscopic studies and Hartree-Fock ab initio calculations of a substituted amide of pyrazine-2-carboxylic acid - $C_{16}H_{18}ClN_3O$. Turk J Chem. 2009;33:633–46.
[41] Karabacak M, Şahin E, Çınar M, Erol I, Kurt M. X-ray, FT-Raman, FT-IR spectra and ab initio HF, DFT calculations of 2-[(5-methylisoxazol-3-yl)amino]-2-oxo-ethyl methacrylate. J Mol Struct. 2008; 886:148–57.
[42] Chesnut D, Phung C. Nuclear magnetic resonance chemical shifts using optimized geometries. J Chem Phys. 1989; 91:6238–45.
[43] Diego MG, Defonsi Lestard ME, Estevez-Hernandes O, Duque J, Reguera E. Quantum chemical studies on molecular structure, spectroscopic (IR, Raman, UV–Vis), NBO and Homo–Lumo analysis of 1-benzyl-3-(2-furoyl) thiourea., Spectrochim Acta A. 2015;145:553–62.
[44] Kavitha E, Sundaraganesan N, Sebastian S, Kurt M. Molecular structure, anharmonic vibrational frequencies and NBO analysis of naphthalene acetic acid by density functional theory calculations. Spectrochim Acta A. 2010;77:612–19.